Analytical Solution Using a Pore Diffusion Model for a Pseudoirreversible Isotherm for the Adsorption of Basic Dye on Silica

GORDON MCKAY

Department of Chemical Engineering
The Queen's University of Belfast
Belfast, N. Ireland

An analytical solution for a two resistance mass transfer model explaining the adsorption of Astrazone Blue dye (Basic Blue 69) onto Sorbsil silica has been developed. The model includes a film mass transfer coefficient, $k_{f_1} = 80 \times 10^{-6}$ cm·s -1, and an internal effective diffusivity, $D_{\text{eff}} = 18 \times 10^{-9}$ cm^2·s^{-1} which controls the internal mass transport processes based on a pore diffusion mechanism.

INTRODUCTION

In recent years the use of adsorption techniques to purify water and waste water has increased considerably. The mass transport within the particles is assumed to be either a pore diffusion (Edeskuty and Amundsen, 1952; Weber and Rumer, 1965; Furusawa and Smith, 1973; Dedrick and Beckmann, 1967) or a homogeneous solid diffusion process (Miller and Clump, 1970; Dryden and Kay, 1954; Mathews and Weber, 1976).

The pore diffusion model outlined in this paper is based on the unreacted shrinking core model (Yagi and Kunii, 1953; Yagi and Kunii, 1961; Levenspiel, 1972; Wen, 1968; Lindman and Simonsson, 1979) and involves a pseudosteady-state approximation. The model has mostly been applied to gas-solid reactions, but a number of liquid-solid systems have been analyzed (Cordell, 1968; Holl and Sontheimer, 1977; Baer and Lewin, 1970; Neretnieks, 1976; Spahn and Schlunder, 1975). In the pore diffusion model there is an adsorption of the adsorbate into the pores with a concurrent distributed adsorption all along the pore wall.

The system reported in this study is the adsorption of Astrazone Blue dye onto Sorbsil silica. The experimental system and some theoretical aspects have been reported previously (McKay and Allen, 1980; McKay et al., 1978; Neretnieks, 1974; Weber, 1978). The assumptions made in the model include: (a) film mass transfer; (b) pore diffusion; (c) irreversible adsorption isotherm; (d) all operating lines terminate at the monolayer; (e) pseudosteady-state approximation; and (f) linear driving force in both film and particle mass transfer.

The silica used was Sorbsil type A supplied by J. Crossfield & Sons, Widnes, and the individual experimental runs are shown in Table 1.

THEORY

Transort Processes

The mass transfer at the external surface layer of the silica particles is given by:

TABLE 1. EXPERIMENTAL RUNS

Run	C_o (mg·dm^{-3})	d_p (cm)	$Y_{e,h}$ (mg·g^{-1})	C_h	M (g)	V (dm^3)	RPM
1	520	0.0605	25	0.481	17	1.7	400
2	410	0.0605	25	0.610	17	1.7	400
3	452	0.0605	25	0.553	17	1.7	400
4	500	0.0605	25	0.375	12.7	1.7	400
5	490	0.0605	25	0.255	8.5	1.7	400
6	480	0.0302	25	0.571	17	1.7	400

$$N(t) = k_f A(C_t - C_{e,t}) \tag{1}$$

The mass transfer within the silica particle through the pores is given by:

$$N(t) = k_p \rho_t A(Y_{e,t} - \bar{Y}_t) \tag{2}$$

The adsorption rate is obtained by graphical differentiation of the C_t vs. time curve, and the differential mass balance is:

$$N(t) = -V \frac{dC_t}{dt} = W \frac{d\bar{Y}_t}{dt} \tag{3}$$

The external mass transfer coefficient can be determined readily (Furusawa and Smith, 1973; Spahn and Schlunder, 1975; McKay and Allen, 1980) and then k_p can be determined by combining Eqs. 1 and 2, and exhibits a time dependence.

$$k_p = \frac{k_f (C_t - C_{e,t})}{\rho_t (Y_{e,t} - \bar{Y}_t)} \tag{4}$$

Determination of Adsorption Rate

A general equation for prediting the adsorption can be made based on certain conditions and assumptions.

(a) The mass transfer from the external water phase is given by Eq. 5.

$$N(t) = 4\pi R^2 k_f (C_t - C_{e,t}) \tag{5}$$

(b) Diffusion in the pore water occurs according to Fick's first law.

$$N(t) = \frac{4\pi D_p}{\left(\frac{1}{r_F} - \frac{1}{R}\right)} C_{e,t} \text{ based on } C_{e,t}/r_F = 0 \tag{6}$$

(c) The velocity of the concentration front is obtained from the mass balance on a spherical element.

$$N(t) = -4\pi r^2_F Y_{e,h} \rho_t \frac{dr_F}{dt} \text{ based on } Y_{e,t}/r_F = Y_{e,h} \tag{7}$$

(d) The average concentration in the silica is given by:

$$\bar{Y}_t = Y_{e,h}\left[1 - \left(\frac{r_F}{R}\right)^3\right] \text{ based on } Y_{e,t}/r_F = Y_{e,h} \tag{8}$$

Since the conditions in Eqs. 6-8 cannot be satisfied simultaneously, a uniform isotherm is assumed and the model is applied where $C_{e,\infty} > C_{e,h}$·$C_{e,h}$ is the threshold concentration for $Y_{e,h}$.

By introducing the following dimensionless parameters,

$$\eta = \frac{\bar{Y}_t}{Y_{e,h}}; \quad \psi = \frac{C_t}{C_o}; \quad \tau = \left[\frac{C_o}{\rho_t Y_{e,h}}\right]\left[\frac{D_p t}{R^2}\right];$$

$$Bi = \frac{k_f R}{D_p} C_h = \frac{Y_{e,h} W}{C_o V}$$

the adsorption rate for a single particle can be expressed as a function of adsorbate concentration in the water phase, ψ, in the adsorbent phase, η, and of the Biot number, Bi, and is represented by Eq. 9.

$$\frac{d\eta}{d\tau} = \frac{3(1 - C_h \cdot \eta)(1 - \eta)^{0.33}}{1 - (1 - Bi^{-1})(1 - \eta)^{0.33}} \tag{9}$$

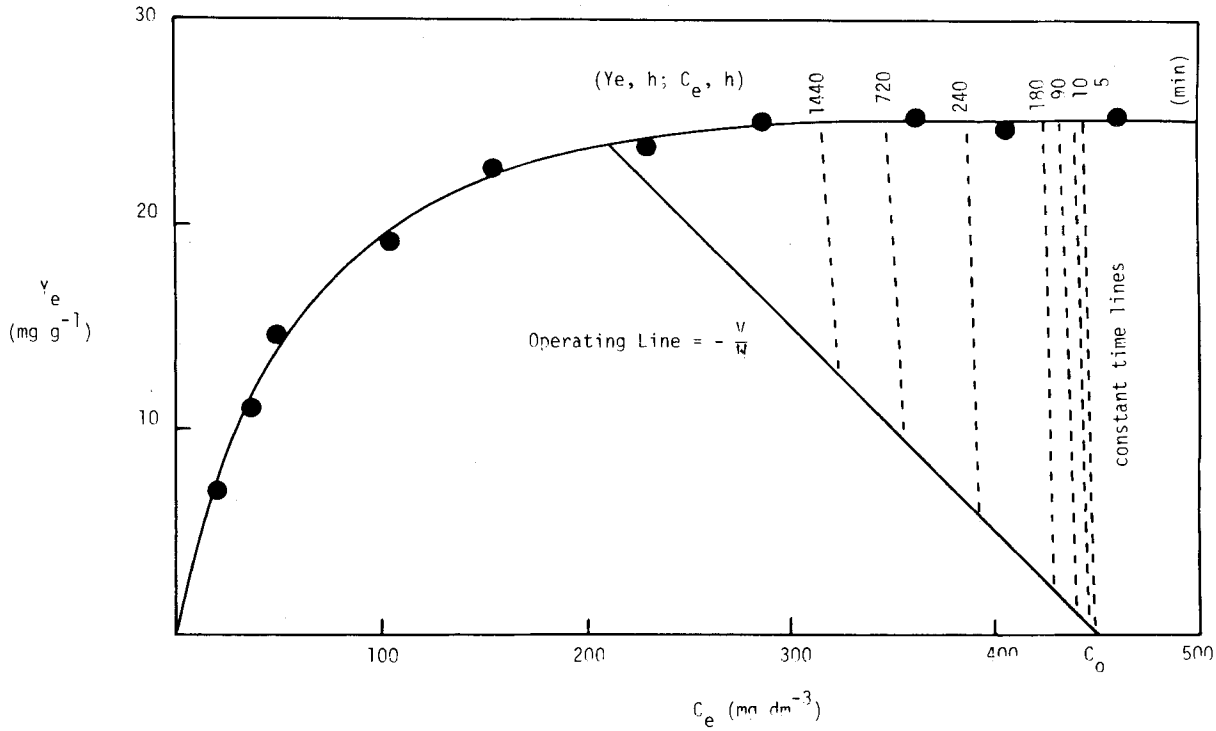

Figure 1. Adsorption of astrazone blue on silica.

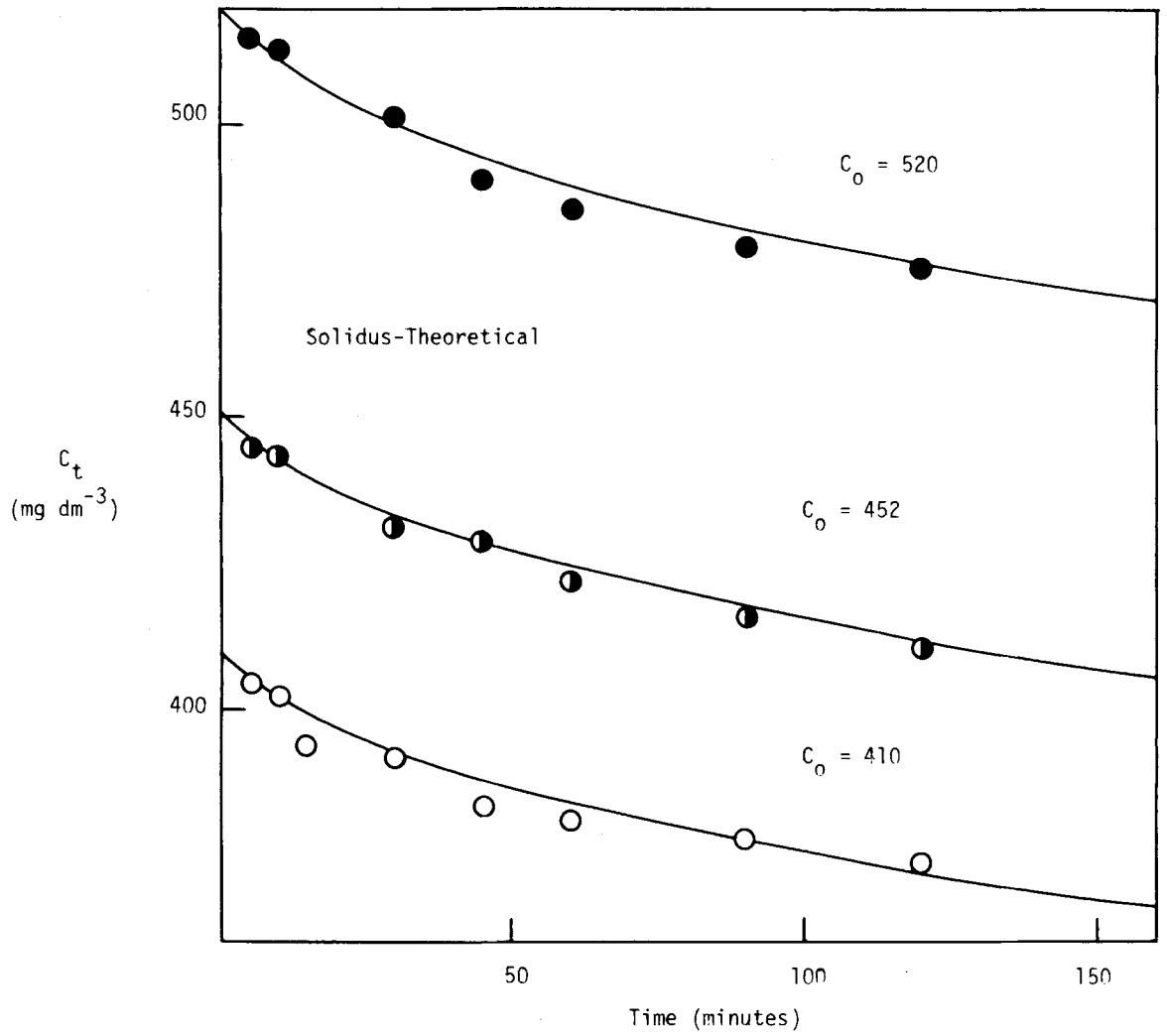

Figure 2. Effect of initial dye concentration.

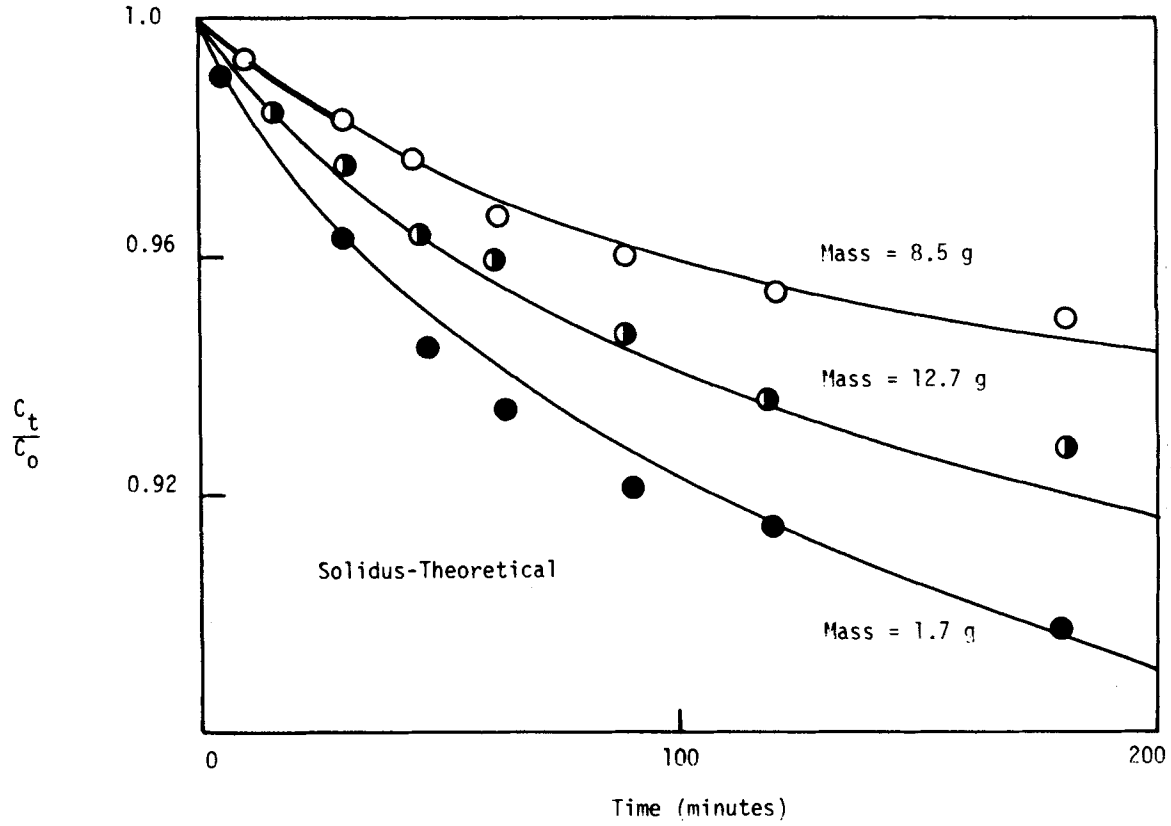

Figure 3. Effect of silica mass.

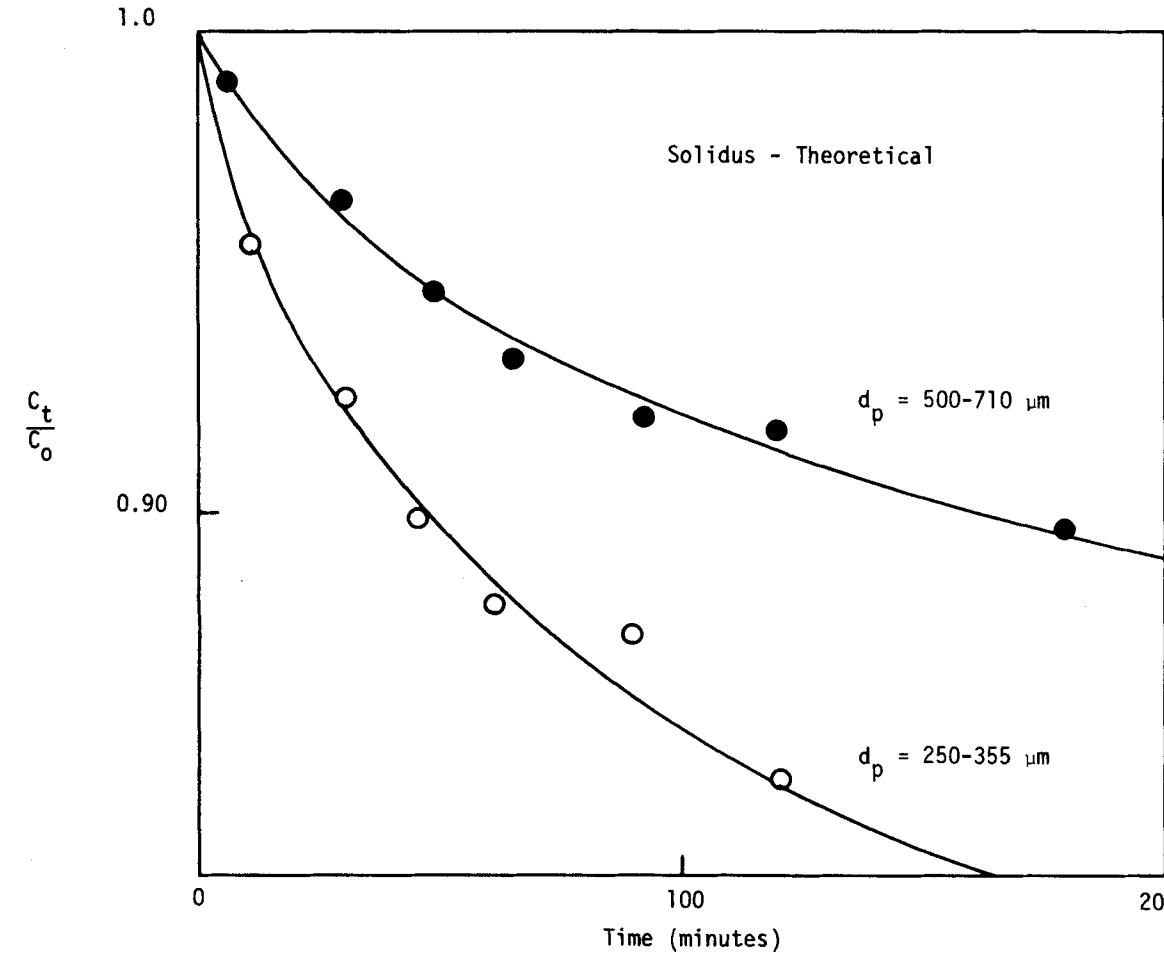

Figure 4. Effect of silica particle size.

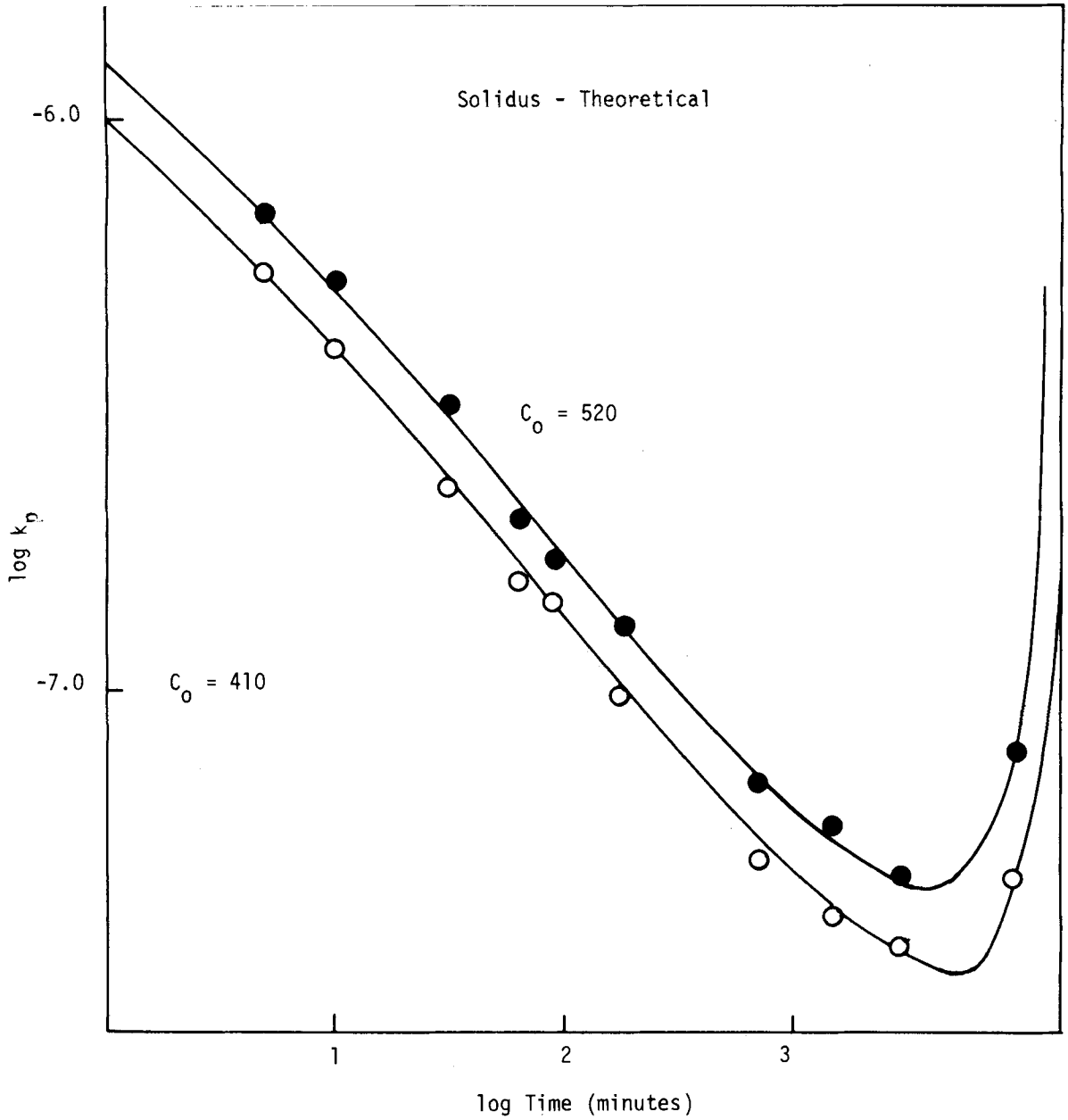

Figure 5. k_p versus time for two initial dye concentrations.

Comparison of Experimental and Theoretical Results

Solution of the previous equations enables experimental and theoretical results to be compared in various forms, for example, η vs. τ, ψ vs. τ, Sh^* vs. τ, where the modified Sherwood number is proportional to the adsorption rate.

$$Sh^* = \frac{1}{3(1-\eta)} \cdot \left(\frac{d\eta}{d\tau}\right) \tag{10}$$

Providing the operating line terminates at the monolayer the system can be treated with a "pseudoirreversible" isotherm approximation, so that,

$$Y_{e,t} - \overline{Y}_t = Y_{e,h} - \overline{Y}_t \tag{11}$$

This assumption allows an analytical solution of Eq. 9 in the following manner. Let

$$B = 1 - \frac{1}{Bi} \tag{12}$$

and

$$X = (1-\eta)^{0.33} \tag{13}$$

Substituting Eqs. 12 and 13, and rearranging; Eq. 9 becomes

$$-\int \frac{X(1-BX)}{[1-C_h(1-X^3)]}\,dX = \int d\tau \tag{14}$$

and if

$$a = \left(\frac{1-C_h}{C_h}\right)^{0.33} \tag{15}$$

$$\frac{1}{C_h}\int \left(\frac{BX^2 - X}{X^3 + a^3}\right) dX = \int d\tau \tag{16}$$

and this can be integrated using partial fractions according to the following form

$$\tau = \frac{1}{6C_h}\left[ln\,\{(IX^3 + a^3I)\}^{(2B-1/a)}\right] + ln\,[\{(IX + aI)^{3/a}\}] - \frac{1}{aC_h 3^{0.5}} \arctan\left[\frac{(2X-a)}{a3^{0.5}}\right] \tag{17}$$

The limits for Eq. 17 are: $\tau = 0$, $\eta = 0$ and $X = 1$ and $\tau = \tau$, $\eta = \eta$ and $X = X$, and inserting these limits into Eq. 17

$$\tau = \frac{1}{6C_h}\left[ln\left[\left[\left|\frac{X^3 + a^3}{1 + a^3}\right|\right]^{(2B-1/a)}\right]\right] + ln\left[\left[\left|\frac{X + a}{1 + a}\right|\right]^{3/a}\right] + \left[\frac{1}{a3^{0.5}C_h}\right]\arctan\left[\frac{2 - a}{a3^{0.5}}\right] - \arctan\left[\frac{2X - a}{a3^{0.5}}\right]\right] \quad (18)$$

Therefore by converting dimensionless time, τ, into real time it is possible to compare experimental and theoretical concentration decay curves.

DISCUSSION

Adsorption Isotherm

The equilibrium isotherm for the adsorption of Astrazone Blue dye on silica is shown in Figure 1. The isotherm follows a Langmuir type of plot forming a monolayer at around $C_e = 200$ mg·dm^{-3}. The analysis of the equilibrium data are given by the following equation.

$$Y_e = 0.5C_e(1 + 0.016\,C_e)^{-1} \quad (19)$$

The assumption of a pseudoirreversible isotherm may be tested numerically using the experimental data and the time dependent k_p values. The results of run 3 have been determined numerically by selecting and testing various D_{eff} values and using Eqs. 1, 2 and 3 and the operating line has been plotted on Figure 1. Graphical differentiation of C_t gives dC_t/dt enabling $N(t)$ to be obtained, hence $Y_{e,\infty}$ and $C_{e,\infty}$ values can be calculated at various constant time values and plotted on Figure 1. A range of results from run 3 are shown on Figure 1 from $t = 5$ min to $t = 1{,}440$ min, all confirming the assumption of a pseudoirreversible isotherm is reasonable, i.e.

$$Y_{e,\infty} = Y_{e,h} \text{ provided } C_e > 20 \text{ mg} \cdot \text{dm}^{-3} \quad (20)$$

Concentration–Time Curves

The analytical solution to the problem of dye adsorption onto silica can be tested by comparing experimental and theoretical results. Equation 18 has been used to generate concentration decay curves for different D_{eff} and different k_f values.

The technique of iterating between D_{eff} and k_f values was adopted using a Fortran program to generate concentration–time curves for a wide range of experimental conditions. It was thus possible to fix a single effective diffusion coefficient, $D_{\text{eff}} = 18 \times 10^{-9}$ cm^2·s^{-1}, and a single film mass transfer coefficient, $k_f = 80 \times 10^{-6}$ cm·s^{-1}, which fit all experimental results with reasonable accuracy. Figures 2, 3 and 4 show the effects of varying: the initial dye concentration, the mass of silica, and the silica particle size range.

Internal Mass Transfer

Using the results and the pseudoirreversibility assumption C_t, Y_t, $C_{e,h}$ and $Y_{e,h}$ are all known at any time, t, and thus using Eqs. 1 and 2 the internal mass transfer coefficients can be computed. The effect of C_o, d_p and silica mass on the time-dependent k_p values are readily obtained. Figure 5 shows the variation of k_p with initial dye concentration. Towards the end of the adsorption runs k_p tends to zero or infinity depending on the liquid/solid ratio expressed in the form of a capacity factor. Thus, $k_p \to 0$ for $C_h > 1$.

In the case of homogeneous solid-phase diffusion k_p is proportional to the square root of the adsorption time. However, for the adsorption of Astrazone Blue dye on silica at long contact times, the k_p values did not follow the ordinary diffusion laws for homogeneous particles. It would appear, therefore, that for much of the adsorption process, the dye is transferred within the pores of the adsorbent particle by molecular diffusion.

CONCLUSIONS

An analytical solution for dye adsorption onto silica has been developed based on film and pore diffusion for the case of an irreversible isotherm. Theoretical concentration decay curves have been compared with experimental data and good agreement obtained for certain design variables; namely, initial dye concentration, adsorbent mass, adsorbent particle size, using a constant film mass transfer coefficient, 80×10^{-6} cm·s^{-1}, and diffusivity of 18×10^{-9} cm^2·s^{-1}. The effective diffusivity may be used in an analytical solution to predict fixed bed breakthrough curves (McKay, 1982).

NOTATION

A = outside surface of particle (cm^2)
a = constant defined by Eq. 15
B = constant defined by Eq. 12
C_t = fluid-phase concentration at time, t (mg·cm^{-3})
$C_{e,t}$ = equilibrium fluid-phase concentration on the particle surface at time, t (mg·cm^{-3})
C_o = initial fluid-phase concentration at time, $t = 0$ (mg·cm^{-3})
D_e = effective diffusion coefficient (cm^2·s^{-1})
D_p = pore diffusion coefficient (cm·s^{-1})
k_f = fluid-phase mass transfer coefficient (cm·s^{-1})
k_p = pore mass transfer coefficient at time, t (cm·s^{-1})
$N(t)$ = adsorption rate at time, t (mg·s^{-1})
r = distance from center of particle, $0 < r < R$ (cm)
R = particle radius (cm)
r_F = radius of concentration front (cm)
t = time (s)
V = volume of batch reactor (cm^3)
W = weight of adsorbent (g)
X = integration variable defined by Eq. 13
$\overline{Y}_t$ = average solid-phase concentration at time, t (mg·g^{-1})
Y_e = equilibrium solid-phase concentration (mg·g^{-1})
$Y_{e,h}$ = equilibrium solid-phase concentration at monolayer capacity (mg·g^{-1})
$Y_{e,t}$ = equilibrium solid-phase concentration at time, t (mg·g^{-1})

Greek Letters

ρ_t = density of solid-phase particles (g·cm^{-3})

Dimensionless Terms

Bi = Biot number
C_h = capacity factor
Sh^* = modified Sherwood number
η = solid-phase concentration
ψ = fluid-phase concentration
τ = dimensionless time

LITERATURE CITED

Baer, N. S., and S. Z. Lewin, "Replacement of Calcite by Fluorite:Kinetic Study," *Amer. Min.*, **55**, p. 466 (1970).

Cordell, G. B., "Reaction Kinetics of the Production of Ammonium Sulphate from Anhydrite," *Ind. Eng. Chem., Proc. Des. Dev.*, **7**, p. 278 (1968).

Dedrick, R. L., and R. B. Beckmann, "Kinetics of Adsorption by Activated Carbon from Dilute Aqueous Solution," *A. I. Chem. E. Symp. Ser.*, No. 74, **63**, p. 68 (1967).

Dryden, C. E., and W. B. Kay, "Kinetics of Batch Adsorption and Desorption," *Ind. Eng. Chem.*, **46**, p. 2294 (1954).

Edeskuty, F. J., and N. R. Amundson, "Effect of Intraparticle Diffusion," *Ind. Eng. Chem.*, **44**, p. 1968 (1952).

Furusawa, T., and J. M. Smith, "Fluid-Particle and Intraparticle Mass

Transport Rates and Slurries," *Ind. Eng. Chem. Fund.*, **12**, p. 197 (1973).
Höll, W., and H. Sontheimer, "Ion Exchange Kinetics of the Prontonation of Weak Acid Ion Exchange Resins," *Chem. Eng. Sci.*, **32**, p. 755 (1977).
Levenspiel, O., *Chemical Reaction Engineering*, Wiley, New York (1972).
Lindman, N., and D. Simonsson, "On the Application of the Shrinking Core Model to Liquid-Solid Reactions," *Chem. Eng. Sci.*, **14**, p. 31 (1979).
Mathews, A. P., and W. J. Weber, Jr., "Effects of External Mass Transfer and Intraparticle Diffusion on Adsorption Rates in Slurry Reactors," *AIChE Symp. Ser.*, No. 166, **73**, p. 91 (1976).
McKay, G., Private Communication.
McKay, G., and S. J. Allen, "Surface Mass Transfer Processes Using Peat as an Adsorbent for Dyestuffs," *Can. J. Chem. Eng.*, **58**, p. 521 (1980).
McKay, G., V. J. P. Poots, and F. Alexander, "Adsorption Kinetics and Diffusional Mass Transfer Processes during Colour Removal from Effluent Using Silica," *Ind. Eng. Chem. Fund.*, **17**, p. 20 (1978).
Miller, C. O., and C. W. Clump, "A Liquid-Phase Adsorption Study of the Rate of Diffusion of Phenol from Aqueous Solution onto Activated Carbon," *AIChE J.*, **16**, p. 169 (1970).
Neretnieks, I., "Adsorption of Components Having a Saturation Isotherm," *Chem. Ing. Techn.*, **46**, No. 18, p. 781 (1974).
Neretnieks, I., "Adsorption in Finite Bath and Countercurrent Flow with Systems Having a Non-Linear Isotherm," *Chem. Eng. Sci.*, **31**, p. 107 (1976).
Neretnieks, I., "Adsorption in Finite Bath and Countercurrent Flow with Systems Having a Concentration Dependant Coefficient of Diffusion," *Chem. Eng. Sci.*, **31**, p. 465 (1976).
Neretnieks, I., "Analysis of Some Adsorption Experiments with Activated Carbon," *Chem. Eng. Sci.*, **31**, p. 1029 (1976).
Spahn, H., and E. U. Schlünder, "The Scale-Up of Activated Carbon Columns for Water Purification, Based on Results from Batch Tests—Part 1," *Chem. Eng. Sci.*, **30**, p. 529 (1975).
Weber, Jr., W. J., and R. R. Rumer, "Intraparticle Transport of Sulphonated Alkylbenzenes in a Porous Solid: Diffusion and Non-Linear Adsorption," *Water Resources Research*, **1**, p. 361 (1965).
Weber, T., "Batch Adsorption for Pore Diffusion with Film Resistance and an Irreversible Isotherm," *Can. J. Chem. Eng.*, **56**, p. 187 (1978).
Wen, C. Y., "Non-Catalytic Heterogeneous Solid-Fluid Reaction Models," *Ind. Eng. Chem.*, **60**, No. 9, p. 34 (1968).
Yagi, S., and D. Kunii, "Proposed Theory of Fluidised Roasting of Sulphide One with Uniform Size," *J. Chem. Soc.* (Japan), **56** 131 (1953).
Yagi, S., and D. Kunii, "Fluidised Solids Reactors with Continuous Solids Feed," *Chem. Eng. Sci.*, **16**, p. 364 (1961).

Manuscript received April 30, 1982; revision received October 28, and accepted November 15, 1982.

Reciprocating Plate Extraction Column As a Cocurrent Mixer

A. E. KARR

Chem-Pro Corp.
Fairfield, NJ 07006

INTRODUCTION

A cocurrent mixer in a mixer-settler extraction system is inherently more efficient than a conventional mixer. In the present work data were obtained in short sections of the Karr Reciprocating Plate Extraction Column (RPEC) employed as a cocurrent mixer. With the system o-xylene-acetic acid-water, stage efficiencies close to 100% were achieved at a total flow rate of 220 $m^3/h \cdot m^2$ when 0.91 m of plate stack operating at an agitation intensity of 1,270 cm/min was employed. At a total flow of 2,010 $m^3/h \cdot m^2$ the stage efficiency was 96.7% at an agitation intensity of 1,778 cm/min.

The data on this system showed:

1. The lower the throughput the higher the efficiency for a given intensity of agitation.
2. The greater the agitation intensity the greater the efficiency.
3. The longer the plate stack the higher the efficiency.

With commercial systems, unlike the o-xylene-acetic acid-water system, it was possible to overmix, which resulted in excessive settling times. This indicates the need to optimize the agitation intensity which is readily achieved in the RPEC.

The flexibility and uniform turbulence in the RPEC should minimize the formation of emulsions while insuring a close approach to equilibrium.

At the ISEC '77 Conference in Toronto Barnea (1977), Orjans, et al. (1977) and Kennedy and Pfalzgraff (1977) showed that multiple mixers in series for use in mixer-settler extraction systems offered advantages, such as improving mixer efficiency and reducing settler volume. The logical extension of this trend is to employ a plug flow mixer, thus Godfrey and Slater (1978) and Merchuk et al. (1980) studied static mixers and packed columns operating in a cocurrent manner.

The Reciprocating Plate Extraction Column has been previously reported by Karr (1959, 1980), Karr and Lo (1971, 1976), and Karr et al. (1980) when employed in a countercurrent manner. In this paper data are presented on short sections of a Reciprocating Plate Extraction Column employed as a cocurrent mixer.

EXPERIMENTAL

The equipment used is shown in Figure 1. 25 mm diameter columns, having lengths of 0.61, 0.91 and 1.22 m were employed. The plates were made of Teflon and were spaced 50 mm apart. A drawing of the plate is shown in Figure 2. Flows were controlled via calibrated rotameters. Both aqueous and solvent streams entered at the bottom of the column. The effluent from the top of the column was run into a 44 L receiver while waiting for equilibrium conditions to be achieved. Then a sample was taken in a 2 L separatory funnel. As soon as clear layers were observed at the top and bottom of the separatory funnel the respective samples were taken for analysis.

O-Xylene-Acetic Acid-Water System

Most of the data were obtained with the o-xylene-acetic acid-water system. This system was selected because it was considered to be a relatively difficult extraction system. Xylene containing approximately 1% acetic acid was extracted with water. The volumetric xylene to water flow ratio was approximately 16 to 1 in all runs. The extraction factor was an average of 2.2 over the range of concentrations studied. The interfacial tension for the system is 26–29 dyne/cm at the exit concentrations of the xylene and aqueous phases.

Phase separation for this system was very rapid. It was nearly complete within 15 seconds and complete within 2 minutes at the highest intensity of agitation.

The results obtained are given in Table I and plotted in Figure 3. In this figure, agitation intensity, the product of stroke length and agitation speed, is plotted against stage efficiency for different lengths of plate stack and throughput. Stage efficiency is the ratio of the change of acetic acid con-